

# Efficient clinical-grade $\gamma$ -retroviral vector purification by high-speed centrifugation for CAR T cell manufacturing

Leila Mekkaoui,<sup>1</sup> Jose G. Tejerizo,<sup>1</sup> Sara Abreu,<sup>1</sup> Lydie Rubat,<sup>1</sup> Aleksandra Nikoniuk,<sup>1</sup> William Macmorland,<sup>1</sup> Claire Horlock,<sup>1</sup> Sofia Matsumoto,<sup>1</sup> Sarah Williams,<sup>1</sup> Koval Smith,<sup>1</sup> Juliet Price,<sup>1</sup> Saket Srivastava,<sup>1</sup> Rehan Hussain,<sup>1</sup> Mohammad Amin Banani,<sup>1</sup> William Day,<sup>1</sup> Elena Stevenson,<sup>1</sup> Meghan Madigan,<sup>2</sup> Jie Chen,<sup>2</sup> Ravin Khinder,<sup>2</sup> Shahed Miah,<sup>2</sup> Simon Walker,<sup>2</sup> Michael Ade-Onojobi,<sup>2</sup> Sabine Dominguez,<sup>2</sup> James Sillibourne,<sup>1</sup> Marianna Sabatino,<sup>1</sup> Vladimir Slepishkin,<sup>1</sup> Farzin Farzaneh,<sup>2</sup> and Martin Pule<sup>1,3</sup>

<sup>1</sup>Autolus Limited, The MediaWorks, 191 Wood Lane, London W12 7FP, UK; <sup>2</sup>Cell and Gene Therapy, Kings (CGT-K), King's College London, London SE5 9NU, UK; <sup>3</sup>Department of Haematology, Cancer Institute, University College London, London WC1E 6BT, UK

**$\gamma$ -Retroviral vectors ( $\gamma$ -RV) are powerful tools for gene therapy applications. Current clinical vectors are produced from stable producer cell lines which require minimal further downstream processing, while purification schemes for  $\gamma$ -RV produced by transient transfection have not been thoroughly investigated. We aimed to develop a method to purify transiently produced  $\gamma$ -RV for early clinical studies. Here, we report a simple one-step purification method by high-speed centrifugation for  $\gamma$ -RV produced by transient transfection for clinical application. High-speed centrifugation enabled the concentration of viral titers in the range of  $10^7$ – $10^8$  TU/mL with >80% overall recovery. Analysis of research-grade concentrated vector revealed sufficient reduction in product- and process-related impurities. Furthermore, product characterization of clinical-grade  $\gamma$ -RV by BioReliance demonstrated two-logs lower impurities per transducing unit compared with regulatory authority-approved stable producer cell line vector for clinical application. In terms of CAR T cell manufacturing, clinical-grade  $\gamma$ -RV produced by transient transfection and purified by high-speed centrifugation was similar to  $\gamma$ -RV produced from a clinical-grade stable producer cell line. This method will be of value for studies using  $\gamma$ -RV to bridge vector supply between early- and late-stage clinical trials.**

## INTRODUCTION

$\gamma$ -Retroviral vectors ( $\gamma$ -RV) derived from Moloney murine leukemia virus (MoMLV) remain the most commonly used integrating vectors for clinical applications.<sup>1</sup> These vectors have an advantage over closely related lentiviral vectors (LV) in that methods to establish high-titer  $\gamma$ -RV producer cell lines are well established and commonly used, while in contrast successful application of stable LV producers in clinical studies is limited. Producer cell lines enable the production of large batches of vector in a cost-

effective manner with little batch-to-batch variation. This advantage is significant when large-scale vector production is required, for instance during large clinical studies or commercial cell therapy manufacture.

The generation of stable producers is a costly and lengthy process,<sup>2</sup> as single-cell clones must first be generated followed by the establishment of a good manufacturing practice (GMP) master cell bank and individualized optimization of vector production.<sup>3–5</sup> Consequently, stable  $\gamma$ -RV producer generation acts as a considerable barrier to early-phase clinical testing of gene therapies, despite potential advantages in subsequent larger clinical studies. In contrast, LV are typically manufactured by transient transfection, which necessitates downstream processing for the removal of impurities such as transfection reagents and residual plasmid DNA. Despite this, transient LV production is quick and simple at the scale of a typical phase I study. Notably, however, transient production scales poorly from practical and economic perspectives compared with  $\gamma$ -RV stable producer vector production, which do not require extensive downstream purification because vectors are free from contaminants such as residual plasmid DNA.

Since most early gene therapy clinical studies fail to meet the predefined endpoints set for progression to the next clinical phase, investigators are motivated to use a vector manufacturing platform which is fast and inexpensive to produce vectors at scale sufficient for early studies. Consequently,  $\gamma$ -RV are less utilized in this setting, and their advantages in large-scale production are infrequently brought to bear for successful therapies. Therefore, a transient transfection method of

Received 19 June 2022; accepted 7 December 2022;  
<https://doi.org/10.1016/j.omtm.2022.12.006>

**Correspondence:** Martin Pule, Autolus Limited, The MediaWorks, 191 Wood Lane, London W12 7FP, UK.

**E-mail:** [m.pule@ucl.ac.uk](mailto:m.pule@ucl.ac.uk)

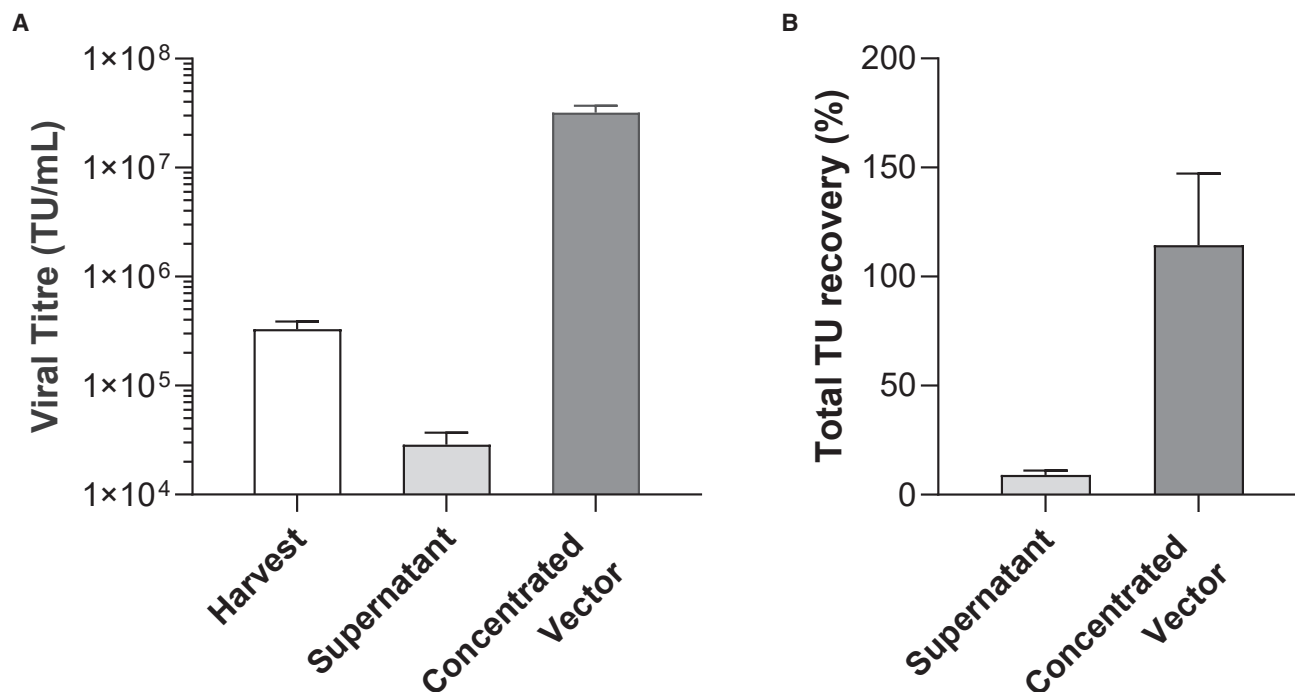


**Figure 1. Concentration of  $\gamma$ -RV by high-speed centrifugation**

$\gamma$ -RV produced by transient transfection was harvested and centrifuged at  $10,000 \times g$  for 20 h at 4°C. The post-centrifugation supernatant was collected, and the concentrated vector pellets were resuspended at a 100 $\times$  volume reduction. (A) Viral titers (transducing unit (TU)/mL) and (B) percentage of TU recovery compared with total TU input in starting harvest material. Data represent mean  $\pm$  SD of three independent experiments.

manufacturing  $\gamma$ -RV utilized in early-phase studies, which could be efficiently bridged to a stable producer cell line for larger confirmatory clinical studies, is desirable: such an approach would have the best of both worlds: rapid vector production for phase I studies with the possibility of using stable cell production for successful therapies.

LV production based on transient transfection typically involves downstream processing methods to remove impurities, with anion exchange chromatography (AEX) being the most applied technique alongside tangential flow filtration (TFF).<sup>6</sup> Little experience with these methods exists with  $\gamma$ -RV produced by transient transfection. The pseudotyping glycoprotein of a viral particle largely defines its stability. LV are typically pseudotyped with the G glycoprotein of vesicular stomatitis virus (VSV-G), which confers high particle stability,<sup>7</sup> and is suited to AEX and TFF. The glycoprotein from the feline endogenous virus RD114 is increasingly used to pseudotype  $\gamma$ -RV, as it has a high tropism to CD34<sup>+</sup> cells and T cells<sup>8</sup> and, unlike VSV-G,<sup>9</sup> lacks cytotoxicity, allowing stable packaging cell generation.<sup>10–13</sup> It also has increased biophysical stability compared with other commonly used glycoproteins such as amphotropic murine leukemia virus and gibbon ape leukemia virus.<sup>14,15</sup>

RD114 has been shown to withstand centrifugal forces ranging from 3,000 to 100,000  $\times g$  with overall recoveries of 40%–

80%.<sup>16–19</sup> However, vector processing by ultracentrifugation can result in co-purification of impurities.<sup>20,21</sup> Here, we investigated the use of simple high-speed centrifugation as a one-step downstream processing method for  $\gamma$ -RV pseudotyped with RD114 produced by transient transfection at a scale sufficient for a typical phase I chimeric antigen receptor (CAR) T cell study.  $\gamma$ -RV were efficiently concentrated with high overall recoveries and reasonable impurity clearance. This method was also investigated as a potential downstream process for clinical-grade  $\gamma$ -RV production for CAR T cell manufacture. We also explored bridging from transient/high-speed centrifuged RD114  $\gamma$ -RV to vector produced from a stable producer cell line in the context of clinical-scale CAR T cell manufacture.

## RESULTS

### High-speed centrifugation results in high overall recovery with concentrated viral titers

A complex but clinically relevant bicistronic CAR T cell cassette expressing CARs<sup>22</sup> (Figure S1) was used in this study. RD114 pseudotyped  $\gamma$ -RV vector was generated by transient transfection of human embryonic kidney (HEK) 293T cells. The feasibility of vector downstream processing by high-speed centrifugation was determined by subjecting 300 mL of  $\gamma$ -RV harvest ( $3.30 \pm 0.57 \times 10^5$  transducing units [TU]/mL) to centrifugation at  $10,000 \times g$  overnight (20 h) at 4°C. A centrifugal force of  $10,000 \times g$  was selected

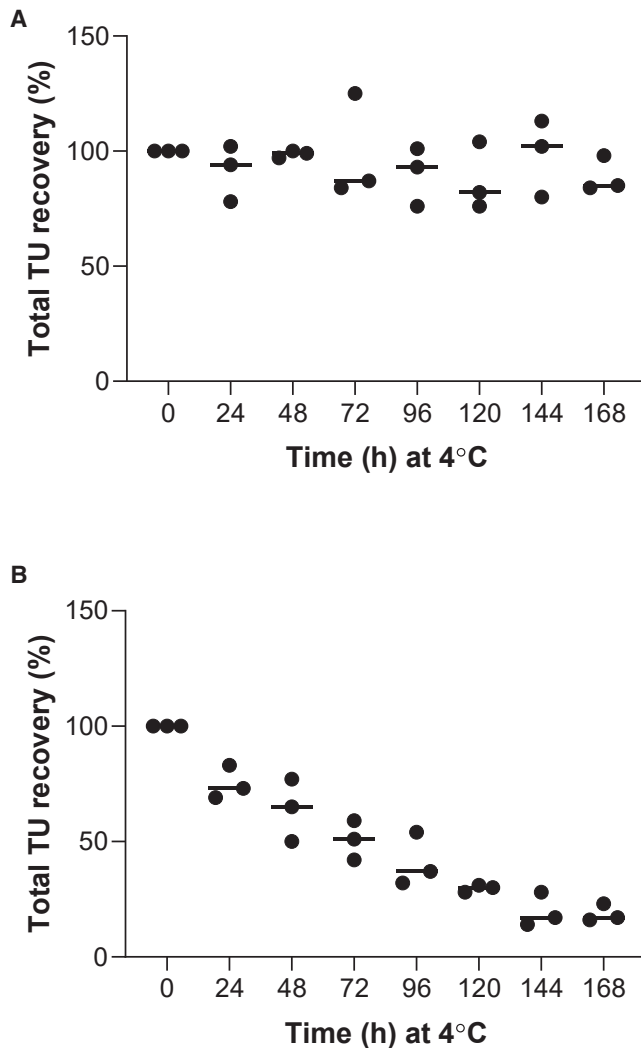


**Figure 2. Stability of unconcentrated and concentrated  $\gamma$ -RV at 4°C**

(A)  $\gamma$ -RV harvest produced by transient transfection and (B) concentrated  $\gamma$ -RV by high-speed centrifugation were incubated at 4°C for up to 168 h. Data are presented as percentage of total TU compared with total TU input at 0 h, with horizontal lines representing mean of three independent experiments.

because this is the highest speed of most fixed-rotor large-scale centrifuges. Supernatant (1 $\times$ ) was collected post centrifugation to determine the efficiency of viral particle sedimentation, and viral pellet (termed concentrated vector) was frozen immediately after resuspension in a 100 $\times$  reduced volume of Opti-MEM and stored at  $-80^{\circ}\text{C}$ . Viral titers were determined for all samples by infectivity of HEK 293T cells (Figure 1A). High-speed centrifugation resulted in concentrated vector with  $3.20 \pm 0.50 \times 10^7$  TU/mL viral titer, corresponding to a 97  $\pm$  15-fold concentration and an overall recovery of 103%  $\pm$  26%, while negligible viral particles were detected in the supernatant ( $2.87 \pm 0.84 \times 10^4$  TU/mL), representing 9%  $\pm$  2% of the overall yield (Figure 1B).

#### Concentrated $\gamma$ -RV exhibits low stability with storage at 4°C

Stability of both unconcentrated and concentrated  $\gamma$ -RV at 4°C would allow flexible process design. To determine stability, unconcentrated harvest and concentrated  $\gamma$ -RV were stored at 4°C for 24, 48, 72, 96, 120, 144, and 168 h and total TU were quantified for up to 7 days. No significant loss in total TU was noted for unconcentrated harvest at 4°C, with 11%  $\pm$  8% reduction from 0 h to 168 h of incubation (Figure 2A).  $\gamma$ -RV concentrated by high-speed centrifugation resuspended in Opti-MEM exhibited lower stability at 4°C, however, as extended incubation resulted in 81%  $\pm$  4% reduction in total TU after 168 h of incubation (Figure 2B).

#### Split centrifugation of $\gamma$ -RV results in concentrated viral titers and high yield

Vector manufacturing for early-phase clinical studies typically produces  $\geq 10$ -L batches. Although certain fixed-angle rotors for large-scale centrifuges can handle such volumes, we explored a split process for facilities with limited centrifugation capacity. First, we determined whether shorter centrifugation was effective by comparing viral particle sedimentation for 8 h or 20 h of centrifugation. Although there was a trend, no statistical differences in residual total TU and concentration of viral titers were observed in both supernatant and concentrated vectors (Figure S2). We then tested a split centrifugation process in which a harvest of 840 mL was split into four batches of 210 mL each and centrifuged separately, stored at 4°C, and pooled at the end of the process (Figures 3A and S3). Corresponding volumes of all fractions are presented in Table S1, and viral titers are shown in Figure 3B. Concentrated vector from each spin (V1 to V4) resulted in viral titers ranging between  $9.08 \pm 2.55 \times 10^6$  TU/mL and  $1.02 \pm 0.20 \times 10^7$  TU/mL, which represent 76  $\pm$  25-fold to 85  $\pm$  22-fold concentration compared with unconcentrated harvest ( $1.21 \pm 0.16 \times 10^5$  TU/mL), and overall recoveries ranging from 77%  $\pm$  25% to 91%  $\pm$  25%, while 12%  $\pm$  5% to 27%  $\pm$  4% of total TU were retained in the supernatants (Figure 3C). These results indicate that high overall recovery can be achieved by split high-speed centrifugation performed over 48 h.

#### Concentrated $\gamma$ -RV product by high-speed centrifugation is of adequate purity

The implementation of any process for early-phase clinical vector production requires adequate removal of process- and product-related impurities. To determine the efficiency of impurity clearance by high-speed centrifugation, four main impurities: HEK 293 host cell proteins (HCP), the nuclease Denarase, bovine serum albumin (BSA), and copies of kanamycin resistance gene (KanR) to determine residual plasmid DNA; were quantified in the starting harvest material, supernatant, and concentrated vectors of the three replicate split centrifugations performed in the previous section (Table 1), as well as the final pooled concentrated vector (Figure S3C). Significant clearances were observed for total HCP ( $\mu\text{g}$ ), Denarase ( $\mu\text{g}$ ), and BSA (mg) in concentrated vectors compared with harvest, with  $\geq 95.89\% \pm 0.77\%$ ,  $\geq 99.82\% \pm 0.06\%$ , and  $\geq 99.89\% \pm 0.04\%$  total reductions, respectively. Plasmid DNA was reduced by  $\geq 35.65\% \pm 0.06\%$  in the four concentrated vectors, with 44.16%  $\pm$  15.60% reduction in the final pooled concentrated vector compared with starting material (Figure S3C). In terms of impurities

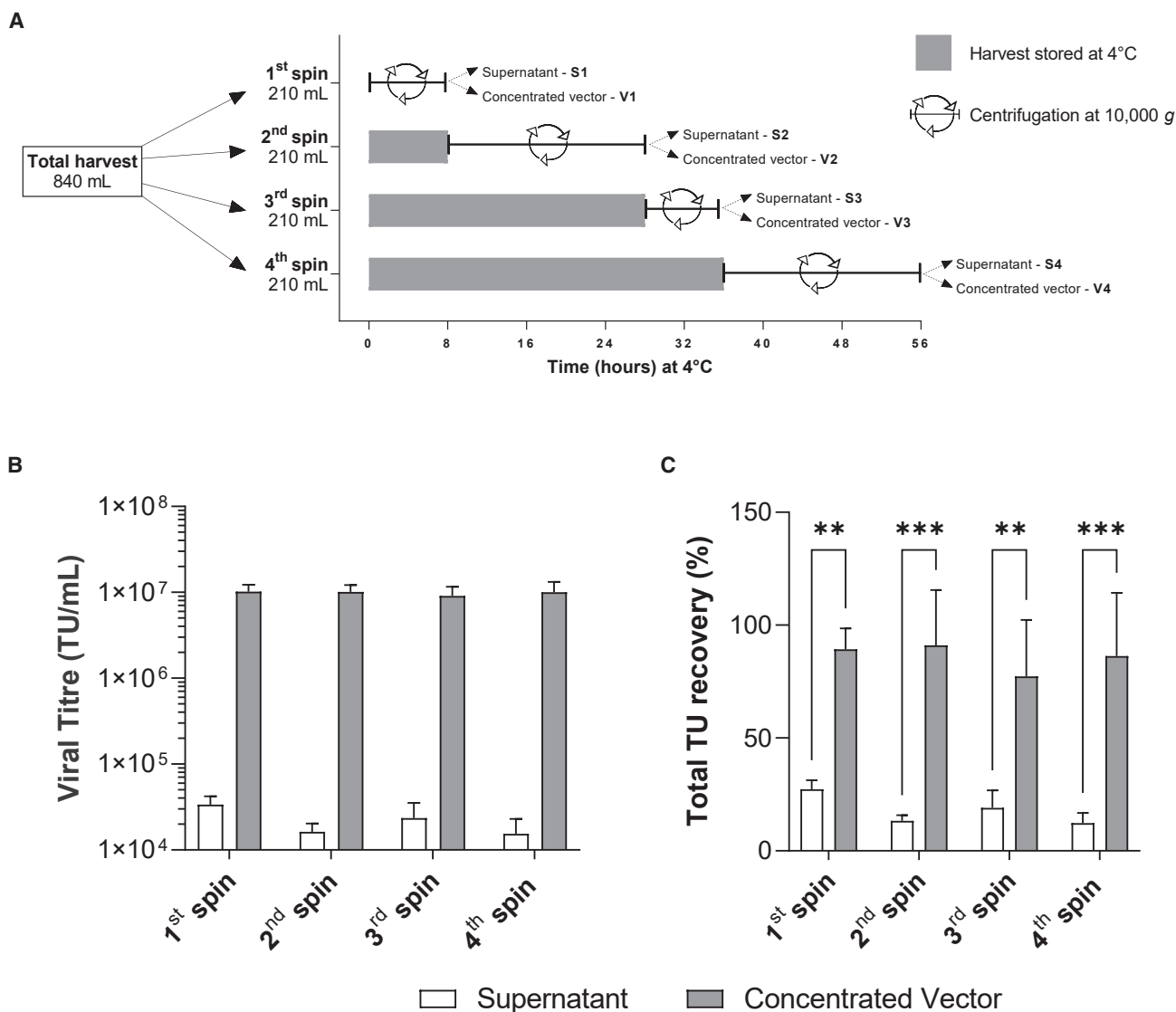


**Figure 3. Concentration of  $\gamma$ -RV by split high-speed centrifugations**

(A) Schematic diagram of split centrifugation protocol over 48 h with detailed sampling strategy. (B) Viral titers (TU/mL) of supernatants 1 $\times$  (S1 to S4) and concentrated vectors 100 $\times$  (V1 to V4) of each of the four centrifugations depicted in (A). (C) Percentage of total TU recovery of concentrated vectors compared with total TU input in starting harvest material per respective high-speed centrifugation. Data in (B) and (C) represent mean  $\pm$  SD of three independent experiments; with \*\* $p < 0.01$  and \*\*\* $p < 0.001$ , two-way ANOVA with Sidak's test for multiple comparisons.

per TU, HCP, Denarase, BSA, and plasmid DNA were reduced by ranges of 97- to 182-fold, 1,975- to 4,787-fold, 2,889- to 8,731-fold, and up to 1.8-fold, respectively, in the four concentrated vectors compared with respective supernatants.

#### **$\gamma$ -RV purification by split high-speed centrifugation is feasible with clinical-grade manufacturing following GMP conditions**

High purity and competitive overall recoveries achieved by split high-speed centrifugation led to transfer of the process to a manufacturing facility following GMP for the purification of a scaled-up harvest batch

of 11 L. A high-titer stable producer cell line that was previously generated for clinical use was used to act as a comparator, and a clinical-grade downstream process was employed to harvest vector from the stable producer. Product characterization of both  $\gamma$ -RV produced by (1) transient transfection followed by purification by high-speed centrifugation (termed Transient) or by (2) a stable producer cell line (termed Stable) were performed by BioReliance, and titers were determined by HEK 293T cell infectivity (Table 2). The full-scale high-speed split centrifugation resulted in a concentrated vector titer of  $3.07 \pm 0.08 \times 10^7$  TU/mL, while the stable producer vector titer was  $1.52 \pm 0.11 \times 10^5$  TU/mL. In

**Table 1. Product and process-related impurity assessment of concentrated  $\gamma$ -RV by split high-speed centrifugation**

Samples	Total impurities (impurities/transducing unit)				
	HCP ( $\mu$ g)	Plasmid DNA (KanR copies)	Denarase ( $\mu$ g)	BSA (mg)	
Harvest per spin	93.03 $\pm$ 8.02 ( $3.65 \pm 0.32 \times 10^{-6}$ )	1.99 $\pm$ 0.60 $\times 10^8$ (1.98 $\pm$ 0.63)	567.21 $\pm$ 33.68 ( $2.23 \pm 0.13 \times 10^{-5}$ )	371.61 $\pm$ 15.96 ( $1.46 \pm 0.06 \times 10^{-5}$ )	
1 <sup>st</sup> spin	S1	91.71 $\pm$ 15.85 ( $1.30 \pm 0.22 \times 10^{-5}$ )	4.79 $\pm$ 1.57 $\times 10^7$ (6.87 $\pm$ 1.64)	573.58 $\pm$ 61.55 ( $8.12 \pm 0.87 \times 10^{-5}$ )	356.79 $\pm$ 13.17 ( $5.05 \pm 0.19 \times 10^{-5}$ )
	V1	3.06 $\pm$ 0.33 ( $1.34 \pm 0.14 \times 10^{-7}$ )	1.21 $\pm$ 0.15 $\times 10^8$ (5.52 $\pm$ 1.81)	0.94 $\pm$ 0.25 ( $4.11 \pm 1.09 \times 10^{-8}$ )	0.40 $\pm$ 0.15 ( $1.75 \pm 0.66 \times 10^{-8}$ )
	<b>Total reduction (%)</b>	<b>96.68 <math>\pm</math> 0.59</b>	<b>35.65 <math>\pm</math> 18.14</b>	<b>99.83 <math>\pm</math> 0.06</b>	<b>99.89 <math>\pm</math> 0.04</b>
2 <sup>nd</sup> spin	S2	96.33 $\pm$ 5.01 ( $2.83 \pm 0.15 \times 10^{-5}$ )	2.60 $\pm$ 1.27 $\times 10^7$ (8.33 $\pm$ 4.93)	552.01 $\pm$ 40.49 ( $1.62 \pm 0.12 \times 10^{-4}$ )	375.32 $\pm$ 14.98 ( $1.10 \pm 0.04 \times 10^{-4}$ )
	V2	3.53 $\pm$ 0.14 ( $1.55 \pm 0.01 \times 10^{-7}$ )	1.00 $\pm$ 0.66 $\times 10^8$ (4.80 $\pm$ 3.47)	1.00 $\pm$ 0.36 ( $4.40 \pm 1.58 \times 10^{-8}$ )	0.45 $\pm$ 0.17 ( $1.97 \pm 0.76 \times 10^{-8}$ )
	<b>Total reduction (%)</b>	<b>96.18 <math>\pm</math> 0.45</b>	<b>53.28 <math>\pm</math> 26.62</b>	<b>99.82 <math>\pm</math> 0.06</b>	<b>99.88 <math>\pm</math> 0.5</b>
3 <sup>rd</sup> spin	S3	89.74 $\pm$ 15.45 ( $1.81 \pm 0.31 \times 10^{-5}$ )	4.89 $\pm$ 3.85 $\times 10^7$ (9.24 $\pm$ 3.50)	548.02 $\pm$ 30.82 ( $1.11 \pm 0.06 \times 10^{-4}$ )	369.05 $\pm$ 22.44 ( $7.46 \pm 0.45 \times 10^{-5}$ )
	V3	2.79 $\pm$ 0.33 ( $1.45 \pm 0.17 \times 10^{-7}$ )	8.45 $\pm$ 2.67 $\times 10^7$ (4.87 $\pm$ 2.98)	0.72 $\pm$ 0.20 ( $3.74 \pm 1.04 \times 10^{-8}$ )	0.28 $\pm$ 0.01 ( $1.43 \pm 0.03 \times 10^{-8}$ )
	<b>Total reduction (%)</b>	<b>96.97 <math>\pm</math> 0.55</b>	<b>57.18 <math>\pm</math> 5.90</b>	<b>99.87 <math>\pm</math> 0.04</b>	<b>99.93 <math>\pm</math> 0.00</b>
4 <sup>th</sup> spin	S4	91.21 $\pm$ 14.02 ( $2.85 \pm 0.43 \times 10^{-5}$ )	1.56 $\pm$ 0.62 $\times 10^7$ (5.21 $\pm$ 1.87)	531.70 $\pm$ 35.56 ( $1.64 \pm 0.11 \times 10^{-4}$ )	347.79 $\pm$ 29.06 ( $1.07 \pm 0.01 \times 10^{-4}$ )
	V4	3.78 $\pm$ 0.46 ( $1.75 \pm 0.21 \times 10^{-7}$ )	1.03 $\pm$ 0.17 $\times 10^8$ (5.20 $\pm$ 2.43)	0.74 $\pm$ 0.25 ( $3.43 \pm 1.16 \times 10^{-8}$ )	0.27 $\pm$ 0.09 ( $1.25 \pm 0.43 \times 10^{-8}$ )
	<b>Total reduction (%)</b>	<b>95.89 <math>\pm</math> 0.77</b>	<b>45.21 <math>\pm</math> 18.43</b>	<b>99.87 <math>\pm</math> 0.05</b>	<b>99.93 <math>\pm</math> 0.03</b>

Table presenting four impurities: HEK 293 host cell proteins (HCP), copies of kanamycin resistance gene (KanR) for residual plasmid DNA, nuclease Denarase, and BSA, which were quantified in starting harvest and then divided by four to obtain impurity concentrations in harvest per split high-speed centrifugation. Impurities were quantified in supernatant fractions (S) and concentrated vectors (V). Total impurities per transducing unit are presented in parentheses. Data represent mean  $\pm$  SD of three independent experiments. Percentages of total reduction in each concentrated vector (V1 to V4) compared with harvest are presented for each split high-speed centrifugation in bold, with the values representing the average total reduction of the three independent purifications  $\pm$ SD.

terms of product specifications, parameters were quantified per TU (rather than volume), as in CAR T cell manufacturing, and the amount of  $\gamma$ -RV added is calculated on the basis of multiplicity of infection (MOI), which is independent of volume. Impurities per TU quantified in the Transient vector were at least two logs lower compared with those detected in the Stable vector, with  $7.49 \times 10^{-4}$  and  $7.04 \times 10^{-2}$  copies/TU of DNA fragments encoding the SV40 large T antigen,  $3.39 \times 10^{-6}$  and  $2.83 \times 10^{-4}$   $\mu$ g/mL of residual BSA,  $6.57 \times 10^{-6}$  and  $2.18 \times 10^{-3}$  ng/mL of residual host cell DNA, and  $7.49 \times 10^{-8}$  and  $7.89 \times 10^{-6}$   $\mu$ g/mL of residual HCP, respectively.

To demonstrate that this process was generalizable, two additional clinical-grade 11-L batches of  $\gamma$ -RV produced by transient transfection for early-phase clinical studies were purified by the same process and characterized by BioReliance (Table S2). These encoded larger, more complex expression cassettes which encode four genes in one open reading frame (lengths: 7.4 kb and 6.8 kb, from LTR [long terminal repeat] to LTR, designated quad-cistronic I and II, respectively) than the bicistronic  $\gamma$ -RV used throughout this study (6.5 kb from LTR to LTR), and their purification by split high-speed centrifugation resulted in viral titers of  $1.44 \times 10^7$  TU/mL and  $1.56 \times 10^8$  TU/mL. Residual product- and process-related impurities per TU were comparable with the impurity profile of the clinical-grade bicistronic  $\gamma$ -RV produced by transient transfection.

#### CAR T cell drug products manufactured with transient and stable $\gamma$ -RV are similar

If an early clinical study using  $\gamma$ -RV produced by transient transfection is successful, our vision is that manufacturing would be bridged

to use  $\gamma$ -RV made from stable producer cell lines. To demonstrate the feasibility of this strategy, equivalence assessment of Transient and Stable  $\gamma$ -RV was performed using a clinically relevant CAR T cell product manufacturing process of three healthy donors in the automated cell processing CliniMACS Prodigy system (Table S3). No statistically significant differences in total viable cells throughout the process were observed between Stable and Transient  $\gamma$ -RV with  $2.93 \pm 0.83 \times 10^9$  and  $3.20 \pm 0.59 \times 10^9$  total cells, respectively at day 8, corresponding to equivalent final T cell fold-expansion of  $29 \pm 8$  and  $31 \pm 6$  (Figures 4A and 4B). Cell viabilities throughout the process for both  $\gamma$ -RV were comparable (Figure 4C). No statistically significant differences in transduction efficiencies were detected for all three donors, with  $45\% \pm 17\%$  and  $47\% \pm 14\%$  CAR-positive cells transduced with Stable and Transient  $\gamma$ -RV, respectively (Figure 4D).

To further demonstrate comparability between  $\gamma$ -RV for clinical application, comprehensive drug product characterization was performed on thawed CAR T cell products which were frozen on day 8, thereby mimicking the manufacturing of patient products for adoptive T cell therapy (Figure 5). In terms of immunophenotyping, no statistically significant differences in T cell subsets were detected in both CD4<sup>+</sup>CAR<sup>+</sup> and CD8<sup>+</sup>CAR<sup>+</sup> compartments (Figure 5A). CD4<sup>+</sup>CAR<sup>+</sup> and CD8<sup>+</sup>CAR<sup>+</sup> compartments for both Stable and Transient  $\gamma$ -RV had comparable activation profiles (Figure 5B). CAR T cells produced with Transient  $\gamma$ -RV did not result in any statistically significant differences in the expression of exhaustion markers compared with cells manufactured with Stable  $\gamma$ -RV, based on the percentage of cells expressing combinations of four exhaustion



**Table 2. Full product characterization of clinical-grade vectors by BioReliance**

Parameter	Method	Specification/result	
		Transient	Stable
Sterility	EP, USP and JP	no growth	no growth
Endotoxin	quantitative, chromogenic assay	<0.05 EU/mL	<0.05 EU/mL
Mycoplasma	USP, EP, PTC 1993	pass (not detected)	pass (not detected)
RCR infectivity	293 detector cells, 5 passages, PG4 S <sup>+</sup> L <sup>-</sup> endpoint	pass (not detected)	pass (not detected)
pH	USP and EP	7.8	7
Osmolality(mOsm/Kg)		294	304
Kanamycin (DNA/TU)	qPCR KAN resistance gene	10.75 ± 0.75	N/A
HEK293 host cell gene targets (copies/TU):	qPCR		
EIA		5.44 ± 0.42 × 10 <sup>-3</sup>	2.52 × 10 <sup>-1</sup>
EIB		6.55 ± 0.30 × 10 <sup>-4</sup>	4.28 × 10 <sup>-1</sup>
SV40 large T antigen		7.49 ± 0.36 × 10 <sup>-4</sup>	7.04 × 10 <sup>-2</sup>
Residual benzonase (ng/TU)	EIA	1.43 × 10 <sup>-7</sup>	N/A
Residual BSA (µg/TU)	ELISA	3.39 ± 0.03 × 10 <sup>-6</sup>	2.83 ± 0.18 × 10 <sup>-4</sup>
Residual human host cell DNA (ng/TU)	qPCR	6.57 × 10 <sup>-6</sup>	2.18 × 10 <sup>-3</sup>
293 HCP (µg/TU)	HEK293 HCP ELISA	7.50 ± 0.65 × 10 <sup>-8</sup>	7.90 × 10 <sup>-6</sup>
Physical titer (µg p30/TU)	p30 ELISA	2.06 ± 0.08 × 10 <sup>-5</sup>	9.87 ± 0.20 × 10 <sup>-5</sup>
Viral titer (TU/mL)	HEK293T infectivity assay	3.07 ± 0.08 × 10 <sup>7</sup>	1.52 ± 0.11 × 10 <sup>5</sup>

Vector product release testing performed by BioReliance of  $\gamma$ -RV produced from stable producer cell line which was not centrifuged (termed "Stable") and  $\gamma$ -RV produced by transient transfection and processed by four split high-speed centrifugations (termed "Transient"). EP, European Pharmacopeia; USP, US Pharmacopeia; PTC 1993, US Food and Drug Administration Points to Consider; RCR, replication competent retrovirus; ELISA, enzyme-linked immunosorbent assay; EIA, enzyme immunoassay.

markers (PD-1, LAG-3, TIGIT, and TIM-3), in both CD4<sup>+</sup>CAR<sup>+</sup> and CD8<sup>+</sup>CAR<sup>+</sup> compartments, with most of the cells expressing none or one exhaustion marker (Figure 5C). CAR T cell potency was investigated and, in line with activation and exhaustion, no statistically significant differences in the cytolytic capacity of cells manufactured with Transient and Stable  $\gamma$ -RV were observed against two target cell lines: Sup-T1 engineered to co-express CD19 and CD22 or Raji cells that endogenously express both antigens (Figure 5D). Accordingly, no statistically significant differences were detected in the secretion of cytokines (interleukin-2 [IL-2], interferon- $\gamma$  [IFN- $\gamma$ ], granzyme B, and tumor necrosis factor  $\alpha$  [TNF- $\alpha$ ]) from CAR T cells manufactured with either  $\gamma$ -RV (Figure 5E).

## DISCUSSION

Here, we report that transient RD114-pseudotyped MoMLV-based  $\gamma$ -RV can be efficiently concentrated and purified using a simple high-speed centrifugation process which combines excellent yield with adequate impurity clearance. In a comparability study,  $\gamma$ -RV produced by transient transfection and purified by high-speed centrifugation was equivalent to vector produced from a clinical-grade stable producer cell line designed for use in an early-phase clinical study for CAR T cell manufacturing. We show that  $\gamma$ -RV produced by transient transfection can be used to make CAR T cells at clinical scale. No differences were observed between CAR T cells manufactured using  $\gamma$ -RV produced by either transient transfection or generated from the stable producer cell line.

The success of engineered immune cell therapy has resulted in an increasing demand for clinical-grade integrating vectors.<sup>23,24</sup> Although there has been an increase in the use of HIV-1-based LV for clinical application,  $\gamma$ -RV are still widely used in the manufacture of CAR T cell therapies,<sup>25</sup> with two approved products using  $\gamma$ -RV for relapsed/refractory diffuse large B cell lymphoma<sup>26</sup> and mantle cell lymphoma.<sup>27</sup> One advantage of  $\gamma$ -RV is the ability to easily generate high-titer stable producer cell lines.<sup>28–30</sup> However, the development of such cell lines is both costly and time consuming, which makes their use unsuited for early-stage clinical studies, given that most of these studies fail. We hypothesized that a clinical-scale transient production process of  $\gamma$ -RV suitable for early studies, which could be bridged to a process utilizing a stable producer cell line vector, would offer investigators the best of both worlds: speed for high-risk early studies and scale for larger confirmatory studies and subsequent commercial application.

Purification schemes for clinical-grade LV produced by transient transfection are well established and involve complex and technical methodology for both process- and product-related impurities removal, such as AEX and TFF, which translate into typical overall recoveries of 30%.<sup>31–33</sup> These purification schemes are not established for clinical-grade  $\gamma$ -RV, as these vectors are typically produced by stable producer cell lines<sup>34–36</sup> which do not require extensive impurity clearance and are often simply clarified by microfiltration to remove cellular debris.<sup>37</sup>

Centrifugation is commonly applied for manufacturing both viral vectors and vaccine as a concentration and intermediate purification step prior to filtration or chromatography-based techniques. Reasonable purification and concentration can be achieved with ultracentrifugation or density gradient centrifugation for  $\gamma$ -RV.<sup>28,38</sup> Continuous flow centrifugation is currently being used for large-scale vaccine manufacture.<sup>39</sup> However, shear effects exerted on viral particles through high centrifugal forces cause structural damage, leading to decreased overall recovery.<sup>40</sup> Given the volume constraint of ultracentrifugation-based methods and the complexity of continuous-flow centrifugation, we hypothesized that high-speed centrifugation as a single step would allow the purification and concentration of  $\gamma$ -RV volumes sufficient for early-phase clinical studies. This would

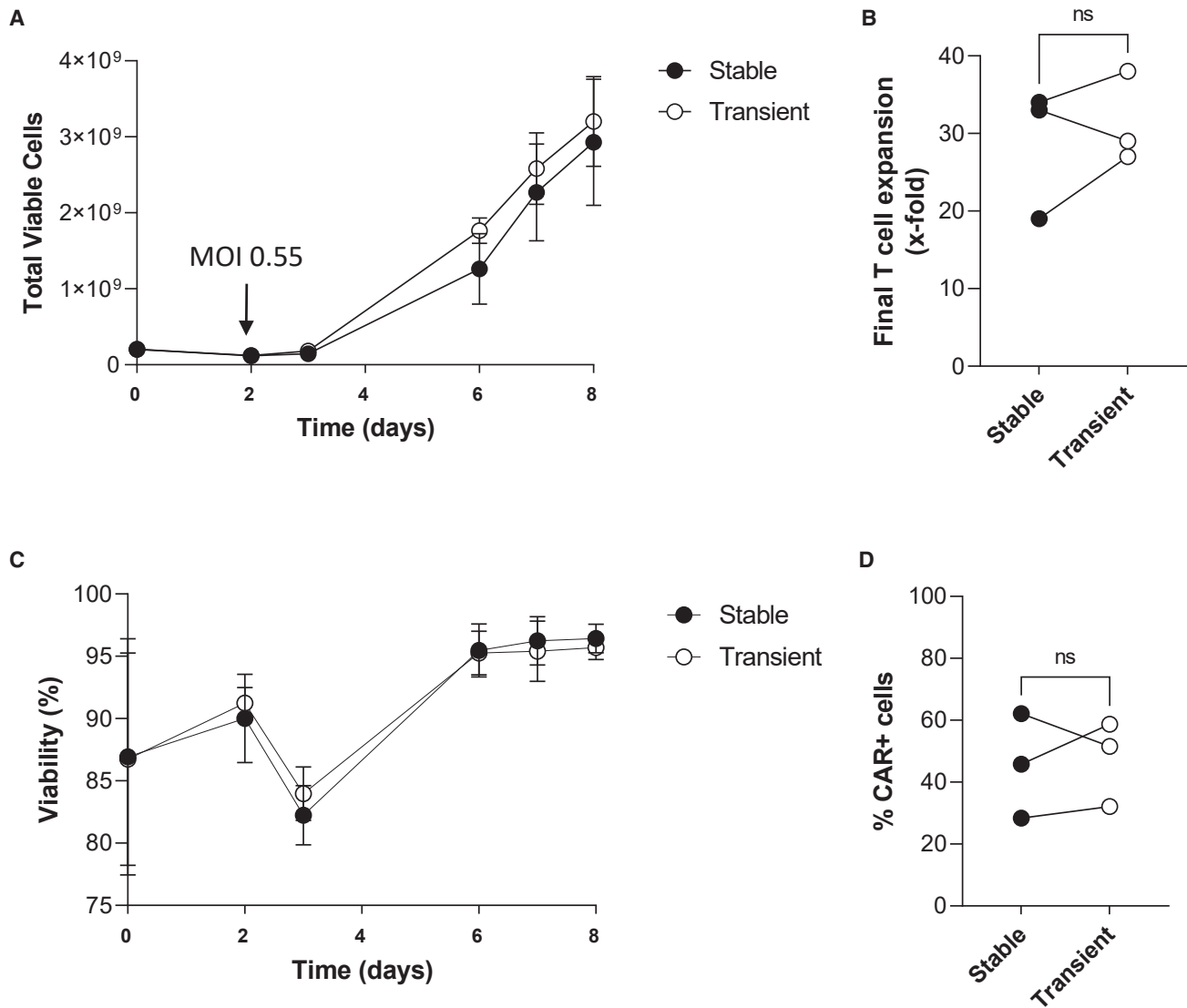


**Figure 4. Automated CAR T cell manufacturing in CliniMACS Prodigy with clinical-grade  $\gamma$ -RV**

Vector produced from stable producer cell line which was not centrifuged (termed “Stable”) and vector produced by transient transfection and processed by four split high-speed centrifugations (termed “Transient”) were used to transduce  $100 \times 10^6$  CD3-positive cells isolated from healthy donors at a clinically relevant MOI of 0.55. (A) Total viable cell number throughout the process, (B) final T cell expansion on day 8, (C) total viability, and (D) transduction efficiencies achieved with each vector and acquired on day 8, which corresponds to day 6 post transduction. Data in (A) and (C) represent mean  $\pm$  SD of three healthy individual donors. Matched donor values are represented in (B) and (D) with ns denoting non-significant p values of 0.5286 and 0.7974, respectively, using a paired t test.

allow a simple and cheap downstream processing method and may not result in co-precipitation of impurities.<sup>41</sup>

Viral particle biostability is conferred by the pseudotyping glycoprotein of choice<sup>7,42,43</sup> as well as the mechanical stability of the viral core.<sup>44</sup> RD114 pseudotyped vector has been reported to be amenable to ultracentrifugation<sup>16,19</sup> and low-speed ( $3,000 \times g$  and  $12,000 \times g$ ) centrifugation,<sup>45–47</sup> with overall recoveries up to 80%. We found that high overall recoveries, with some exceeding 100% of starting material, were achieved by a single round of centrifugation, highlighting

the increased biophysical stability of RD114 pseudotyped MoMLV-based  $\gamma$ -RV. Recoveries greater than 100% are likely caused by the removal of inhibitory factors, such as soluble envelope proteins during centrifugation.<sup>48</sup> Moreover, single centrifugations for either 8 h or 20 h can result in overall recoveries of  $91\% \pm 25\%$  with  $76 \pm 25$ -fold concentration in viral titers, in line with published reports.<sup>49,50</sup> Split centrifugations can also be performed if centrifuge capacity is limiting, resulting in concentrated viral titers in the  $10^7$ – $10^8$  TU/mL range of three clinical-grade RD114 pseudotyped  $\gamma$ -RV expressing multicistronic expression cassettes.

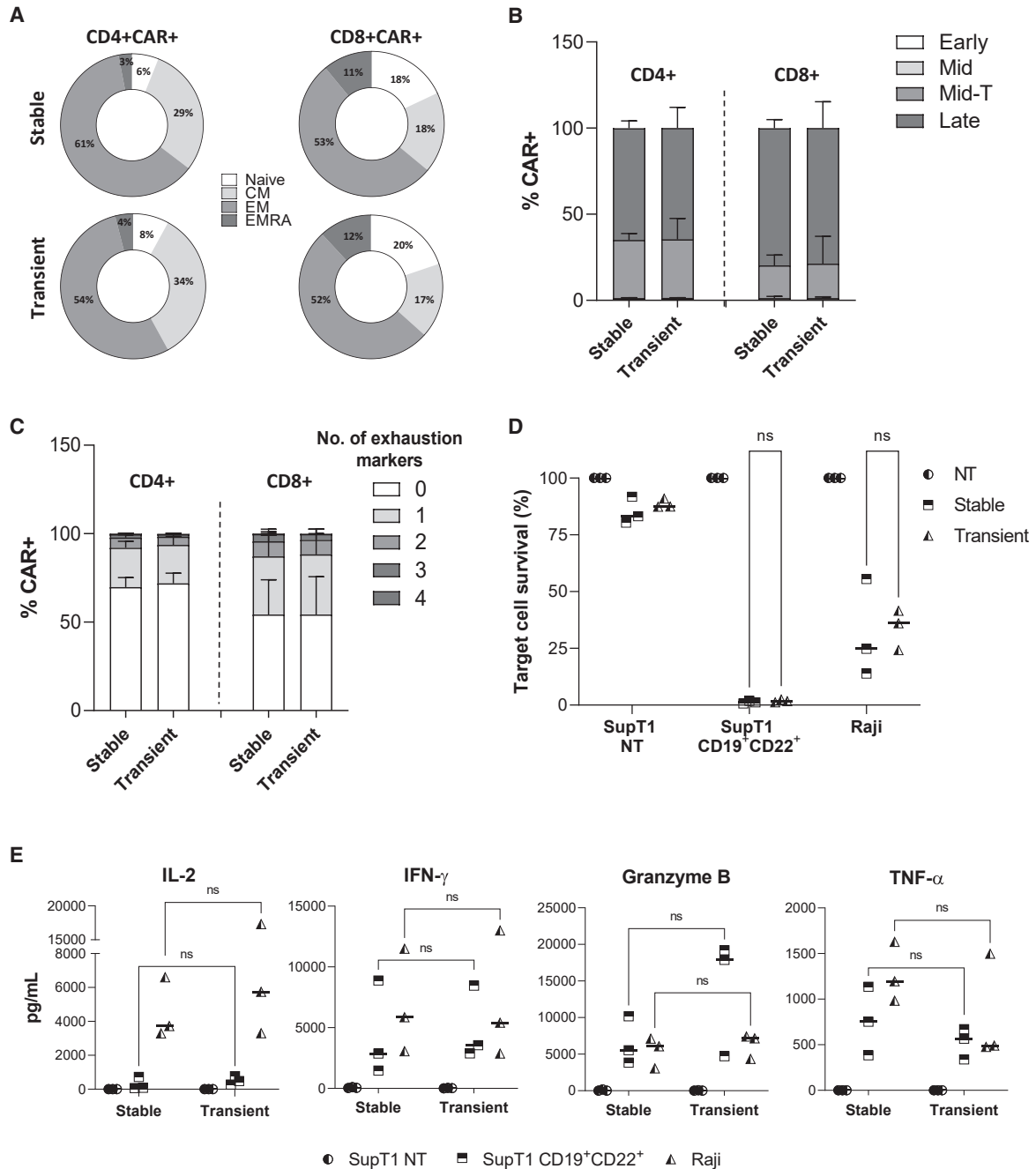


**Figure 5. Comprehensive CAR T cell product characterization**

(A) T cell subset phenotyping of CAR T cells transduced with  $\gamma$ -RV produced from stable producer cell line which was not centrifuged (termed "Stable") and  $\gamma$ -RV produced by transient transfection and processed by four split high-speed centrifugations (termed "Transient") by flow cytometric analysis as part of whole for CD4<sup>+</sup> and CD8<sup>+</sup> compartments; with naive T cells (Naive; CD45RA<sup>+</sup>CCR7<sup>+</sup>CD62L<sup>+</sup>CD27<sup>+</sup>), central memory T cells (CM; CD45RA<sup>-</sup>CCR7<sup>+</sup>CD62L<sup>+</sup>CD27<sup>+</sup>), effector memory T cells (EM; CD45RA<sup>-</sup>CCR7<sup>-</sup>CD62L<sup>-</sup>CD27<sup>+</sup>), and terminally differentiated effector memory T cells (EMRA; CD45RA<sup>+</sup>CCR7<sup>-</sup>CD62L<sup>-</sup>CD27<sup>-</sup>). (B) Activation analysis of CD4<sup>+</sup> and CD8<sup>+</sup> CAR T cells based on surface expression of CD25 and HLADR and categorized into four distinct activation subsets: early activation classified as CD25<sup>-</sup>HLADR<sup>-</sup>, middle activation classified as CD25<sup>+</sup>HLADR<sup>-</sup>, middle-transition activation classified as CD25<sup>+</sup>HLADR<sup>+</sup>, and late activation classified as CD25<sup>-</sup>HLADR<sup>+</sup>. (C) Exhaustion analysis of CD4<sup>+</sup> and CD8<sup>+</sup> CAR T cells based on the number of exhaustion markers (PD-1, LAG-3, TIM-3, and TIGIT) expressed per cell. Data in (A), (B), and (C) represent mean  $\pm$  SD of three independent experiments performed with three healthy individual donors. (D) Cytotoxicity of CAR T cells determined by co-culturing non-transduced (NT) T cells and CAR T cells transduced with either stable or transient  $\gamma$ -RV with NT SupT1, SupT1 engineered to co-express CD19 and CD22 (SupT1 CD19<sup>+</sup>CD22<sup>+</sup>), and wild-type Raji cells

(legend continued on next page)



The use of the centrifugation process we describe here is not ideal in GMP manufacturing because it is an open process, whereas a closed downstream process is desirable. Therefore, work is ongoing to adapt high-speed centrifugation into a closed system. This can be achieved by using weldable caps for centrifugation bottles alongside precision dip tubes that can be used to withdraw suspended vector pellets, enabling aseptic vector harvest transfer. Further work adapting continuous centrifugation to  $\gamma$ -RV purification may release the bottleneck of large-volume centrifugation in a closed system. This would also enable the concentration of  $\gamma$ -RV produced by transfection-based methods or from stable producer cell lines if higher purity and viral titers are required. Further improvements in viral titers for both systems can be achieved by deleting RD114's receptor from HEK 293T cells, thereby eliminating superinfection during vector production.<sup>51</sup>

An important consideration when designing any downstream process is stability of vectors, which was explored in this study. Unmanipulated, RD114  $\gamma$ -RV produced by transient transfection was highly stable at 4°C for up to 7 days, in line with published reports.<sup>16</sup> Storage of concentrated  $\gamma$ -RV at 4°C resulted in gradual decrease in infectivity. This has been previously observed for both  $\gamma$ -RV<sup>41</sup> and LV.<sup>52</sup> However, as many standard large-scale centrifuges can accommodate up to 10 L, concentrated  $\gamma$ -RV may not require storage at 4°C and their gradual loss of infectivity is not a limitation. Future work is required to determine whether optimization of a final buffer formulation might confer enhanced stability as it is impacted by a variety of chemical<sup>53</sup> and physical<sup>54</sup> factors. A comprehensive examination of the effects of different excipients<sup>55</sup> on the stability of  $\gamma$ -RV may increase process flexibility further and is worthy of future study.

High-speed centrifugation resulted in efficient clearance of HCP, Denarase, and BSA impurities with >95% reductions using research-grade  $\gamma$ -RV. This was observed with both centrifugation times tested in this study, indicating that a centrifugation speed of 10,000 × *g* for a minimum of 8 h co-sediments negligible amounts of these contaminants with viral particles. However, centrifugation resulted in a reduction of ~45% of residual plasmid DNA, which equated to a range between 1 and 16 copies of plasmid per TU across several purifications. Clinical-grade  $\gamma$ -RV purified by centrifugation exhibited two-logs lower residual impurities per TU compared with clinical-grade vector generated from the stable producer cell line that was designed for clinical use.<sup>22</sup> Further in-process analysis of vector quality is required by determining physical particle over TU ratios throughout high-speed centrifugation.

The feasibility of bridging transient concentrated  $\gamma$ -RV by centrifugation to vector from a stable cell line was tested in the context of CAR T cell manufacturing. This is required from a regulatory perspective, as any change in the process during clinical development after initial clinical studies must be validated for equivalence of final drug prod-

uct. CAR T cell drug products exhibited a high degree of similarity in terms of viability, expansion, gene transfer efficiency, and immunophenotyping as well as cytotoxic potency.

In conclusion, we describe a simple method for purifying RD114-pseudotyped  $\gamma$ -RV by high-speed centrifugation, which results in high overall recovery of concentrated viral titers. CAR T cell drug products manufactured with concentrated  $\gamma$ -RV are equivalent to those manufactured with vector from stable producer cell lines, thereby enabling faster early clinical study development while maintaining the subsequent advantages of large-scale  $\gamma$ -RV production by producer cell lines. We hope that this process will facilitate more widespread use of  $\gamma$ -RV in early-phase studies.

## MATERIALS AND METHODS

### Cell lines

HEK 293T/17 (ATCC, CRL-11268) cell line was cultured in Iscove's modified Dulbecco's medium (IMDM) (Lonza, cat. no. BE12-726F) supplemented with 10% fetal calf serum (FCS; Biosera, cat. no. FB 1001/500) and 2 mM GlutaMAX (Gibco, cat. no. 35050061) at 37°C with 5% CO<sub>2</sub>. Cells were passaged 1:4–1:10 when cell density reached 75%–85% confluence using trypsin-EDTA solution (Sigma). Sup-T1 (ATCC, CRL-1942) cell line was cultured in Roswell Park Memorial institute (RPMI) 1640 medium (Lonza, cat. no. BE12-702F) supplemented with 10% FCS and 2 mM GlutaMAX at 37°C with 5% CO<sub>2</sub>. Cells were passaged 1:4–1:10 when cell density reached 75%–85%.

### Plasmids and transient vector production

Bicistronic vectors were produced by triple transient transfection of HEK 293T cells using the following three plasmids at 1:1.5:28.6 ratio: (1) codon-optimized Moloney GagPol driven by a CMV promoter; (2) codon-optimized RD114 envelope driven by a ferritin promoter; and (3) a retroviral backbone with a cassette expressing two CARs against CD19 and CD22 separated by a self-cleaving 2A peptide derived from *Thosea asigna* virus capsid protein (Figure S1A). Eighteen to 24 hours post transfection the culture medium was changed with the addition of 50 U/mL of Denarase (c-LEcta) and 1 mM sodium butyrate (Sigma-Aldrich, cat. no. B5887). Vector supernatants were collected 48 h after transfection and clarified by centrifugation at 400 × *g* for 5 min to remove cellular debris, followed by 0.45  $\mu$ m microfiltration (Millipore, cat. no. S2HVVU05RE). Viral supernatants were either kept on ice for further use or snap-frozen and stored at –80°C for later use. All plasmids carried a KanR gene. For the runs performed according to GMP, ccc-grade (covalently closed circular and supercoiled DNA of high purity for advanced requirements) plasmids were used that were manufactured by PlasmidFactory (Germany). Plasmid sequences can be requested from the corresponding author.

---

at 1:4 effector/target ratio for 72 h. Percentages of target cell survival are presented, which were normalized to non-specific killing measured in co-cultures with NT T cells for each target. (E) Production of IL-2, INF- $\gamma$ , granzyme B, and TNF- $\alpha$  quantified in culture medium 72 h post co-culture. Horizontal lines in (D) and (E) represent mean of three healthy individual donors with ns denoting non-significant p value of 0.9964 for SupT1 CD19<sup>+</sup>CD22<sup>+</sup> between stable and transient and p value of 0.9247 for Raji cells between stable and transient, two-way ANOVA with Tukey's test for multiple comparisons.

### Generation of Sup-T1-expressing CD19 and CD22 antigens

Sup-T1 cells were seeded in precoated retronectin 24-well non-tissue culture-treated plates at  $3 \times 10^5$  cells per well with transient  $\gamma$ -RV supernatant carrying human CD19 and CD22 antigens. Transduced cells (SupT1 CD19<sup>+</sup>CD22<sup>+</sup>) were harvested 72 h later and recovered by culturing in serum supplemented RPMI for two passages before use as target cell line.

### Vector production from clinical-grade stable producer cell line

$\gamma$ -RV stable producer cell line based on HEK 293T cells was generated by transient transfection of packaging plasmids and bicistronic transfer vector followed by antibiotic selection (Figure S4). Monoclonality of functional producer clones was achieved by limited dilution of polyclonal population. Once a clone was characterized and stability determined, cells were seeded at  $1.10 \times 10^4$  cells/cm<sup>2</sup> with 0.158 mL/cm<sup>2</sup> of IMDM supplemented with 10% qualified FCS (Gibco, cat. no. 10091148). Culture medium was exchanged 24 h later to TexMACS GMP medium (Miltenyi Biotec, cat. no. 170-076-306) with 0.158 mL/cm<sup>2</sup>. Vector harvests were collected 96 h later, clarified by first centrifugation at  $1,500 \times g$  for 15 min followed by 0.45  $\mu$ m microfiltration (Millipore, cat. no. MPHL20CL3) and then by sterile filtration through 0.22  $\mu$ m (Millipore, cat. no. MPGL1GCL3) before snap-freezing and storage at  $-80^\circ\text{C}$ .

### High-speed centrifugation of research-grade and clinical-grade $\gamma$ -RV produced by transient transfection

$\gamma$ -RV-containing harvest (0.1–11 L) was stored at  $4^\circ\text{C}$ , and 0.25–1 L of vector was added into either flat-bottom 1 L bottles or to conical 250 mL bottles and spun at  $10,000 \times g$  for 8–20 h at  $4^\circ\text{C}$  with an acceleration at 9 and deceleration 2 in a fixed-angle

for 1 h for optimal dissociation. Subsequently, Opti-MEM was pipetted gently to resuspend the pellet and avoid bubble formation. Concentrated vectors were not subjected to sterile filtration by 0.22  $\mu$ m and were either (1) aliquoted, snap-frozen, and stored at  $-80^\circ\text{C}$  or (2) left at  $4^\circ\text{C}$  if more than one spin was performed until all products were pooled together and snap-frozen before storage at  $-80^\circ\text{C}$ . Biosafety testing and product-specific characterization of clinical-grade vectors presented in Tables 2 and S2 were performed by BioReliance.

### Viral vector titration and staining for bicistronic cassette expression

Functional titers were determined by transduction of HEK 293T cells.  $1 \times 10^4$  cells were seeded per well in a flat-bottom 96-well plate. 12.5  $\mu$ L of thawed vectors subjected to a 4-fold serial dilution were added onto cells with 8  $\mu$ g/mL polybrene supplemented in the culture medium and incubated at  $37^\circ\text{C}$  with 5% CO<sub>2</sub> for 72 h. Transduced cells were identified for double CAR expression with an anti-idiotypic antibody specific for the anti-CD19 binder fused to murine IgG2A (binder generated in-house and produced by Evitria) and soluble biotinylated human CD22 (Acrobiosystems, cat. no. SI2-H82F8), followed by secondary staining with Alexa Fluor 647-conjugated goat anti-murine IgG2A antibody (Thermo Fisher Scientific, cat. no. A-21241) and phycoerythrin-conjugates streptavidin (BioLegend, cat. no. 405203), respectively, along with a viability dye for live cell gating (fixable viability stain 780; BD, cat. no. 565388). Expression of both CARs were measured by flow cytometry 3 days post transduction of HEK 293T cells on an LSRFortessa X-20 and analyzed using FlowJo software. Functional titers were determined using the following equation with the double CAR-positive population (Figure S1B) previously gated on live cell populations:

$$\text{Titer} \left( \frac{\text{Transducing units (TU)}}{\text{mL}} \right) = \left( \frac{\left( \frac{\% \text{ transduction efficiency}}{100} \right) \times \text{no. of cells at transduction}}{\text{vector volume}} \right) \times \text{dilution factor}$$

rotor bucket using a Sorvall BIOS centrifuge (Thermo Fisher Scientific). Clinical-grade  $\gamma$ -RV were produced in a full-scale manufacturing run in which 11 L of  $\gamma$ -RV harvest produced by transient transfection was clarified by 0.45  $\mu$ m microfiltration and then processed in four split high-speed centrifugations at  $10,000 \times g$  over 2 days, whereby each day 2.75 L of transient vector was processed for 8 h followed by an overnight centrifugation of another 2.75 L for 20 h. Upon completion of each spin, residual supernatants were gently collected so as not to dislodge the pellets. This step is crucial to ensure increased recovery, as the pellets can be loosely attached to the inside of the bottles. Vector pellets were then gently suspended in Opti-MEM (Thermo Fisher Scientific, cat. no. 31985062) with 100 $\times$  volume reduction and left on ice

Conditions resulting in transduction efficiencies between 1% and 20% were used for titer calculation to ensure linearity of transgene integration.

### Host cell protein quantification

Total HCP were measured by ELISA with a HEK293 HCP kit (Cygnus Technologies, cat. no. F6505). The manufacturer's protocol was followed with diluent buffer (Cygnus, cat. no. I028-500). Analyzed samples were diluted 4-fold ranging from 1:4 to 1:256, and absorbances were measured using a Varioskan LUX multimode microplate reader analyzed using SkanIt software (Thermo Fisher Scientific).

### BSA quantification

Detection of BSA was performed using the bovine albumin kit from Bethyl Laboratories (E11-113) as per manufacturer's protocol. Harvest and concentrated vector product were diluted 4-fold and 3-fold, respectively. Absorbances were measured using a Varioskan LUX multimode microplate reader analyzed using SkanIt software.

### Residual plasmid quantification

Residual kanamycin plasmid contamination was analyzed using the resDNASEQ Quantitative Plasmid DNA—Kanamycin Resistance Gene kit (Thermo Fisher, cat. no. A50460) after nucleic acid extraction using the PrepSEQ Nucleic Acid Samples Preparation kit (Thermo Fisher, cat. no. A50485). The manufacturer's protocols were followed. Samples were diluted 1:10 for the harvest and supernatant and 1:1,000 for the concentrated vectors based on assay optimization before extraction. 21,100 copies of kanamycin resistance plasmid control were spiked into each sample prior of extraction. qPCR plates were measured and analyzed using the Applied Biosystems QuantStudio 7 Flex system. Extraction recoveries between 76% and 110% were considered for data analysis.

### Denarase quantification

Detection of the nuclease was performed using the Denarase ELISA kit from c-LEcta (cat. no. 41901-1) as per manufacturer's instructions. Samples were analyzed in a 4-fold dilution ranging from 1:4 to 1:256, and absorbances were measured at 450 nm using a Varioskan LUX multimode microplate reader analyzed using SkanIt software.

### Clinical-grade T cell transduction using CliniMACS prodigy

Peripheral blood mononuclear cells were collected from healthy donors and frozen. Thawed cells were rested overnight, and T cells were activated with anti-CD3 and anti-CD28 antibodies nanomatrix TransAct (Miltenyi Biotec). Cells were transduced 48 h later with either  $\gamma$ -RV produced from stable producer cells or by a transient transfection process followed by high-speed centrifugation, with an MOI of 0.55. Cells were expanded until day 8, cultured in complete growth medium supplemented with 3% human serum albumin (Octapharma) and human IL-15 and IL-7 (Miltenyi Biotec) cytokines, and cryopreserved thereafter.

### T cell subset phenotype analysis

Extended phenotyping analysis was performed using a 16-color flow cytometry panel developed to measure transformed CAR T cell product differentiation, activation, and exhaustion within both the CD4 (BD, cat. no. 612887) and CD8 (BD, cat. no. 612942) compartments.

Cells were stained for surface markers and viability (fixable viability stain 780; BD, cat. no. 565388), then fixed and permeabilized using the eBioscience Foxp3/Transcription Factor Staining Buffer Set (00-5523-00) following the manufacturer's instructions, and stained thereafter for intracellular markers. Post-staining samples were subsequently acquired on an LSR Fortessa X20 (BD Biosciences). Phenotypic analysis was performed using the software FCS Express 7 (De Novo Software, CA, USA). FMO (fluorescence-minus-one) controls,

acquired alongside the samples, were used for the following markers: CD45RA (BD, cat. no. 566114), CCR7 (BD, cat. no. 741833), CAR T, HLA-DR (BD, cat. no. 564040), CD25 (BD, cat. no. 563701), PD-1 (BD, cat. no. 561272), LAG3 (BD, cat. no. 369308), TIM-3 (BD, cat. no. 565566), TIGIT (Invitrogen, cat. no. 46-9500-42), CD62L (BD, cat. no. 563701), CD27 (BD, cat. no. 741833), CD3 (BD, cat. no. 340440), and CD2 (BioLegend, cat. no. 300224) to assess positive/negative gating limit position.

### Cytotoxicity assay

Cytolytic activity of transduced T cells was assessed by co-culturing  $5 \times 10^4$  anti-CD19/anti-CD22 CAR T cells with three target cells (non-transduced SupT1, SupT1 transduced with CD19 and CD22, and Raji cells) at 1:4 effector/target ratios in flat-bottom 96-well plates. Specific killing was determined by quantification of viable targets via flow cytometry 72 h later by staining co-cultures with a viability dye (fixable viability stain 780; BD, cat. no. 565388) and antibodies against CD3 (BioLegend, cat. no. 34816) and CD2 (BioLegend, cat. no. C36950). This allows for target discrimination from effector cells because, unlike the latter, target cells are negative for both CD3 and CD2 expression. Culture medium was harvested and analyzed for cytokine secretion using a multianalyte simple plex assay performed using the multianalyte assay on Ella (ProteinSimple), customized to quantify the following cytokines: IL-2, IFN- $\gamma$ , Granzyme B, and TNF- $\alpha$ . Non-transduced T cells were used as control in the same effector/target ratios.

### Statistical analysis

One-way and two-way ANOVA were used for comparison of means of three or more groups with one and two variables present, respectively. Paired t test analysis was used for the comparison of means of two groups with one variable present. Generation of graphs and statistical analysis were performed using GraphPad Prism 9.3.1.

### DATA AVAILABILITY

The data that support the findings of this study are available from the corresponding author upon reasonable request.

### SUPPLEMENTAL INFORMATION

Supplemental information can be found online at <https://doi.org/10.1016/j.omtm.2022.12.006>.

### ACKNOWLEDGMENTS

M.P. is supported by the UK National Health Service Biomedical Research Centre at University College London Hospitals. Graphical abstract created with [BioRender.com](https://www.biorender.com).

### AUTHOR CONTRIBUTIONS

Conceptualization, L.M., J.S., M.S., V.S., F.F., and M.P.; methodology, L.M.; investigation, L.M., J.G.T., S.A., S. Matsumoto, L.R., A.N., W.M., C.H., S. Williams, K.S., J.P., S.S., R.H., M.A.B., E.S., S.D., M.M., J.C., R.K., S. Miah, S. Walker, M.A.-O., and W.D.; writing – original draft; L.M.; writing – review & editing, M.P. and J.S.

## DECLARATION OF INTERESTS

L.M., J.G.T., S.A., A.N., W.M., S. Williams, S.S., R.H., M.A.B., E.S., J.S., W.D., and M.P. own stock or stock options in Autolus Ltd as employees. S. Matsumoto, L.R., C.H., K.S., J.P., M.S., and V.S. are previous employees of Autolus Ltd. No other authors declare conflict of interest.

## REFERENCES

- Ginn, S.L., Amaya, A.K., Alexander, I.E., Edelstein, M., and Abedi, M.R. (2018). Gene therapy clinical trials worldwide to 2017: an update. *J. Gene Med.* 20, e3015. <https://doi.org/10.1002/jgm.3015>.
- Coffin, J.M., Hughes, S.H., and Varmus, H.E. (1997). *Principles of Retroviral Vector Design* (Cold Spring Harbor Laboratory Press).
- Cruz, P.E., Almeida, J.S., Murphy, P.N., Moreira, J.L., and Carrondo, M.J. (2000). Modeling retrovirus production for gene therapy. 1. Determination of optimal bio-reaction mode and harvest strategy. *Biotechnol. Prog.* 16, 213–221. <https://doi.org/10.1021/bp9901466>.
- Sheridan, P.L., Bodner, M., Lynn, A., Phuong, T.K., DePolo, N.J., de la Vega, D.J., Jr., O'Dea, J., Nguyen, K., McCormack, J.E., Driver, D.A., et al. (2000). Generation of retroviral packaging and producer cell lines for large-scale vector production and clinical application: improved safety and high titer. *Mol. Ther.* 2, 262–275. <https://doi.org/10.1006/mthe.2000.0123>.
- Wikström, K., Blomberg, P., and Islam, K.B. (2004). Clinical grade vector production: analysis of yield, stability, and storage of GMP-produced retroviral vectors for gene therapy. *Biotechnol. Prog.* 20, 1198–1203. <https://doi.org/10.1021/bp030065g>.
- Merten, O.-W., Schweizer, M., Chahal, P., and Kamen, A. (2014). Manufacturing of viral vectors: part II. Downstream processing and safety aspects. *Pharm. Bioprocess.* 2, 237–251.
- Burns, J.C., Friedmann, T., Driever, W., Burrascano, M., and Yee, J.K. (1993). Vesicular stomatitis virus G glycoprotein pseudotyped retroviral vectors: concentration to very high titer and efficient gene transfer into mammalian and nonmammalian cells. *Proc. Natl. Acad. Sci. USA* 90, 8033–8037.
- Kelly, P.F., Vandergriff, J., Nathwani, A., Nienhuis, A.W., and Vanin, E.F. (2000). Highly efficient gene transfer into cord blood nonobese diabetic/severe combined immunodeficiency repopulating cells by oncoretroviral vector particles pseudotyped with the feline endogenous retrovirus (RD114) envelope protein. *Blood* 96, 1206–1214.
- Hoffmann, M., Wu, Y.-J., Gerber, M., Berger-Rentsch, M., Heimrich, B., Schwemmler, M., and Zimmer, G. (2010). Fusion-active glycoprotein G mediates the cytotoxicity of vesicular stomatitis virus M mutants lacking host shut-off activity. *J. Gen. Virol.* 91, 2782–2793. <https://doi.org/10.1099/vir.0.023978-0>.
- Cosset, F.L., Takeuchi, Y., Battini, J.L., Weiss, R.A., and Collins, M.K. (1995). High-titer packaging cells producing recombinant retroviruses resistant to human serum. *J. Virol.* 69, 7430–7436.
- Ward, M., Sattler, R., Grossman, I.R., Bell, A.J., Skerrett, D., Baxi, L., and Bank, A. (2003). A stable murine-based RD114 retroviral packaging line efficiently transduces human hematopoietic cells. *Mol. Ther.* 8, 804–812.
- Ghani, K., Wang, X., de Campos-Lima, P.O., Olszewska, M., Kamen, A., Rivière, I., and Caruso, M. (2009). Efficient human hematopoietic cell transduction using RD114- and GALV-pseudotyped retroviral vectors produced in suspension and serum-free media. *Hum. Gene Ther.* 20, 966–974. <https://doi.org/10.1089/hum.2009.001>.
- Feldman, S.A., Xu, H., Black, M.A., Park, T.S., Robbins, P.F., Kochenderfer, J.N., Morgan, R.A., and Rosenberg, S.A. (2014). Use of the piggyBac transposon to create stable packaging cell lines for the production of clinical-grade self-inactivating  $\gamma$ -retroviral vectors. *Hum. Gene Ther. Methods* 25, 253–260. <https://doi.org/10.1089/hgtb.2014.071>.
- Neff, T., Peterson, L.J., Morris, J.C., Thompson, J., Zhang, X., Horn, P.A., Thomasson, B.M., and Kiem, H.-P. (2004). Efficient gene transfer to hematopoietic repopulating cells using concentrated RD114-pseudotype vectors produced by human packaging cells. *Mol. Ther.* 9, 157–159. <https://doi.org/10.1016/j.yimthe.2003.11.011>.
- Strang, B.L., Ikeda, Y., Cosset, F.-L., Collins, M.K.L., and Takeuchi, Y. (2004). Characterization of HIV-1 vectors with gammaretrovirus envelope glycoproteins produced from stable packaging cells. *Gene Ther.* 11, 591–598. <https://doi.org/10.1038/sj.gt.3302189>.
- Gatlin, J., Melkus, M.W., Padgett, A., Kelly, P.F., and Garcia, J.V. (2001). Engraftment of NOD/SCID mice with human CD34+ cells transduced by concentrated oncoretroviral vector particles pseudotyped with the feline endogenous retrovirus (RD114) envelope protein. *J. Virol.* 75, 9995–9999. <https://doi.org/10.1128/JVI.75.20.9995-9999.2001>.
- Kelly, P.F., Carrington, J., Nathwani, A., and Vanin, E.F. (2001). RD114-pseudotyped oncoretroviral vectors. Biological and physical properties. *Ann. N. Y. Acad. Sci.* 938, 262–276. discussion 276–277.
- Horn, P.A., Morris, J.C., Peterson, L.J., Thomasson, B.M., Kurre, P., and Kiem, H.-P. (2002). 66. Highly efficient gene transfer into macaque repopulating cells using concentrated RD114-pseudotype vector. *Mol. Ther.* 5, S24. [https://doi.org/10.1016/S1525-0016\(16\)42896-0](https://doi.org/10.1016/S1525-0016(16)42896-0).
- Brenner, S., Whiting-Theobald, N.L., Linton, G.F., Holmes, K.L., Anderson-Cohen, M., Kelly, P.F., Vanin, E.F., Pilon, A.M., Bodine, D.M., Horwitz, M.E., and Malech, H.L. (2003). Concentrated RD114-pseudotyped MFGS-gp91phox vector achieves high levels of functional correction of the chronic granulomatous disease oxidase defect in NOD/SCID/beta -microglobulin-/- repopulating mobilized human peripheral blood CD34+ cells. *Blood* 102, 2789–2797. <https://doi.org/10.1182/blood-2002-05-1482>.
- Bess, J.W., Gorelick, R.J., Bosche, W.J., Henderson, L.E., and Arthur, L.O. (1997). Microvesicles are a source of contaminating cellular proteins found in purified HIV-1 preparations. *Virology* 230, 134–144. <https://doi.org/10.1006/viro.1997.8499>.
- Reiser, J. (2000). Production and concentration of pseudotyped HIV-1-based gene transfer vectors. *Gene Ther.* 7, 910–913. <https://doi.org/10.1038/sj.gt.3301188>.
- Cordoba, S., Onuoha, S., Thomas, S., Pignataro, D.S., Hough, R., Ghorashian, S., Vora, A., Bonney, D., Veys, P., Rao, K., et al. (2021). CAR T cells with dual targeting of CD19 and CD22 in pediatric and young adult patients with relapsed or refractory B cell acute lymphoblastic leukemia: a phase 1 trial. *Nat. Med.* 27, 1797–1805. <https://doi.org/10.1038/s41591-021-01497-1>.
- Levine, B.L., Miskin, J., Wonnacott, K., and Keir, C. (2017). Global manufacturing of CAR T cell therapy. *Mol. Ther. Methods Clin. Dev.* 4, 92–101. <https://doi.org/10.1016/j.omtm.2016.12.006>.
- Rafiq, S., Hackett, C.S., and Brentjens, R.J. (2020). Engineering strategies to overcome the current roadblocks in CAR T cell therapy. *Nat. Rev. Clin. Oncol.* 17, 147–167. <https://doi.org/10.1038/s41571-019-0297-y>.
- Mo, F., and Mamonkin, M. (2020). Generation of chimeric antigen receptor T cells using gammaretroviral vectors. *Methods Mol. Biol.* 2086, 119–130. [https://doi.org/10.1007/978-1-0716-0146-4\\_8](https://doi.org/10.1007/978-1-0716-0146-4_8).
- Neelapu, S.S., Locke, F.L., Bartlett, N.L., Lekakis, L.J., Miklos, D.B., Jacobson, C.A., Braunschweig, I., Oluwole, O.O., Siddiqi, T., Lin, Y., et al. (2017). Axicabtagene ciloleucel CAR T-cell therapy in refractory large B-cell lymphoma. *N. Engl. J. Med.* 377, 2531–2544. <https://doi.org/10.1056/NEJMoa1707447>.
- Wang, M., Munoz, J., Goy, A., Locke, F.L., Jacobson, C.A., Hill, B.T., Timmerman, J.M., Holmes, H., Jaglowski, S., Flinn, I.W., et al. (2020). KTE-X19 CAR T-cell therapy in relapsed or refractory mantle-cell lymphoma. *N. Engl. J. Med.* 382, 1331–1342. <https://doi.org/10.1056/NEJMoa1914347>.
- Ory, D.S., Neugeboren, B.A., and Mulligan, R.C. (1996). A stable human-derived packaging cell line for production of high titer retrovirus/vesicular stomatitis virus G pseudotypes. *Proc. Natl. Acad. Sci. USA* 93, 11400–11406.
- Ikeda, Y., Takeuchi, Y., Martin, F., Cosset, F.-L., Mitrophanous, K., and Collins, M. (2003). Continuous high-titer HIV-1 vector production. *Nat. Biotechnol.* 21, 569–572. <https://doi.org/10.1038/nbt815>.
- Sanber, K.S., Knight, S.B., Stephen, S.L., Bailey, R., Escors, D., Minshull, J., Santilli, G., Thrasher, A.J., Collins, M.K., and Takeuchi, Y. (2015). Construction of stable packaging cell lines for clinical lentiviral vector production. *Sci. Rep.* 5, 9021. <https://doi.org/10.1038/srep09021>.
- Merten, O.-W., Hebben, M., and Bovolenta, C. (2016). Production of lentiviral vectors. *Mol. Ther. Methods Clin. Dev.* 3, 16017. <https://doi.org/10.1038/mtm.2016.17>.



32. van der Loo, J.C.M., and Wright, J.F. (2016). Progress and challenges in viral vector manufacturing. *Hum. Mol. Genet.* 25, R42–R52. <https://doi.org/10.1093/hmg/ddv451>.
33. Dropulic, B., Slepishkin, V., Chang, N., Gan, Y., Jiang, B., Deausen, E., Berlinger, D., Binder, G., Andre, K., and Humeau, L. (2003). Large-scale purification of a lentiviral vector by size exclusion chromatography or Mustang Q ion exchange capsule. *Bioprocess J.* 2, 89–95.
34. Wang, X., Olszewska, M., Qu, J., Wasielewska, T., Bartido, S., Hermetet, G., Sadelain, M., and Rivière, I. (2015). Large-scale clinical-grade retroviral vector production in a fixed-bed bioreactor. *J. Immunother.* 38, 127–135. <https://doi.org/10.1097/CJI.000000000000072>.
35. Boztug, K., Schmidt, M., Schwarzer, A., Banerjee, P.P., Diez, I.A., Dewey, R.A., Böhm, M., Nowrouzi, A., Ball, C.R., Glimm, H., et al. (2010). Stem-cell gene therapy for the wiskott-aldrich syndrome. *N. Engl. J. Med.* 363, 1918–1927. <https://doi.org/10.1056/NEJMoa1003548>.
36. Feldman, S.A., Goff, S.L., Xu, H., Black, M.A., Kochenderfer, J.N., Johnson, L.A., Yang, J.C., Wang, Q., Parkhurst, M.R., Cross, S., et al. (2011). Rapid production of clinical-grade gammaretroviral vectors in expanded surface roller bottles using a “modified” step-filtration process for clearance of packaging cells. *Hum. Gene Ther.* 22, 107–115. <https://doi.org/10.1089/hum.2010.064>.
37. Straathof, K., Flutter, B., Wallace, R., Jain, N., Loka, T., Depani, S., Wright, G., Thomas, S., Cheung, G.W.-K., Gileadi, T., et al. (2020). Antitumor activity without on-target off-tumor toxicity of GD2–chimeric antigen receptor T cells in patients with neuroblastoma. *Sci. Transl. Med.* 12, eabd6169. <https://doi.org/10.1126/scitranslmed.abd6169>.
38. Segura, M.d.L.M., Garnier, A., and Kamen, A. (2006). Purification and characterization of retrovirus vector particles by rate zonal ultracentrifugation. *J. Virol. Methods* 133, 82–91. <https://doi.org/10.1016/j.jviromet.2005.10.030>.
39. Minh, A.D., and Kamen, A.A. (2021). Critical assessment of purification and analytical Technologies for enveloped viral vector and vaccine processing and their current limitations in resolving Co-expressed extracellular vesicles. *Vaccines* 9, 823. <https://doi.org/10.3390/vaccines9080823>.
40. Morenweiser, R. (2005). Downstream processing of viral vectors and vaccines. *Gene Ther.* 12, S103–S110. <https://doi.org/10.1038/sj.gt.3302624>.
41. Ichim, C.V., and Wells, R.A. (2011). Generation of high-titer viral preparations by concentration using successive rounds of ultracentrifugation. *J. Transl. Med.* 9, 137. <https://doi.org/10.1186/1479-5876-9-137>.
42. Beer, C., Meyer, A., Müller, K., and Wirth, M. (2003). The temperature stability of mouse retroviruses depends on the cholesterol levels of viral lipid shell and cellular plasma membrane. *Virology* 308, 137–146. [https://doi.org/10.1016/s0042-6822\(02\)00087-9](https://doi.org/10.1016/s0042-6822(02)00087-9).
43. Segura, M.d.L.M., Kamen, A., and Garnier, A. (2006). Downstream processing of oncoretroviral and lentiviral gene therapy vectors. *Biotechnol. Adv.* 24, 321–337. <https://doi.org/10.1016/j.biotechadv.2005.12.001>.
44. Kim, S.H., and Lim, K.I. (2017). Stability of retroviral vectors against ultracentrifugation is determined by the viral internal core and envelope proteins used for pseudotyping. *Mol. Cells* 40, 339–345. <https://doi.org/10.14348/molcells.2017.0043>.
45. McNeish, I.A., Green, N.K., Gilligan, M.G., Ford, M.J., Mautner, V., Young, L.S., Kerr, D.J., and Searle, P.F. (1998). Virus directed enzyme prodrug therapy for ovarian and pancreatic cancer using retrovirally delivered E. coli nitroreductase and CB1954. *Gene Ther.* 5, 1061–1069. <https://doi.org/10.1038/sj.gt.3300744>.
46. Bowles, N.E., Eisensmith, R.C., Mohuidin, R., Pyron, M., and Woo, S.L. (1996). A simple and efficient method for the concentration and purification of recombinant retrovirus for increased hepatocyte transduction in vivo. *Hum. Gene Ther.* 7, 1735–1742. <https://doi.org/10.1089/hum.1996.7.14-1735>.
47. Relander, T., Johansson, M., Olsson, K., Ikeda, Y., Takeuchi, Y., Collins, M., and Richter, J. (2005). Gene transfer to repopulating human CD34+ cells using amphotropic-GALV- or RD114-pseudotyped HIV-1-based vectors from stable producer cells. *Mol. Ther.* 11, 452–459. <https://doi.org/10.1016/j.ymthe.2004.10.014>.
48. Andreadis, S.T., Roth, C.M., Le Doux, J.M., Morgan, J.R., and Yarmush, M.L. (1999). Large-scale processing of recombinant retroviruses for gene therapy. *Biotechnol. Prog.* 15, 1–11. <https://doi.org/10.1021/bp980106m>.
49. Seppen, J., Kimmel, R.J., and Osborne, W.R. (1997). Serum-free production, concentration and purification of recombinant retroviruses. *Biotechniques* 23, 788–790. <https://doi.org/10.2144/97235bm04>.
50. Bell, A.J., Fegen, D., Ward, M., and Bank, A. (2010). RD114 envelope proteins provide an effective and versatile approach to pseudotype lentiviral vectors. *Exp. Biol. Med.* 235, 1269–1276. <https://doi.org/10.1258/ebm.2010.010053>.
51. Labenski, V., Suerth, J.D., Barczak, E., Heckl, D., Levy, C., Bernadin, O., Charpentier, E., Williams, D.A., Fehse, B., Verhoeven, E., and Schambach, A. (2016). Alpharetroviral self-inactivating vectors produced by a superinfection-resistant stable packaging cell line allow genetic modification of primary human T lymphocytes. *Biomaterials* 97, 97–109. <https://doi.org/10.1016/j.biomaterials.2016.04.019>.
52. Jiang, W., Hua, R., Wei, M., Li, C., Qiu, Z., Yang, X., and Zhang, C. (2015). An optimized method for high-titer lentivirus preparations without ultracentrifugation. *Sci. Rep.* 5, 13875. <https://doi.org/10.1038/srep13875>.
53. Pham, L., Ye, H., Cosset, F.L., Russell, S.J., and Peng, K.W. (2001). Concentration of viral vectors by co-precipitation with calcium phosphate. *J. Gene Med.* 3, 188–194. [https://doi.org/10.1002/1521-2254\(2000\)9999:9999::AID-JGM159>3.0.CO;2](https://doi.org/10.1002/1521-2254(2000)9999:9999::AID-JGM159>3.0.CO;2).
54. Pradhan, S., Varsani, A., Leff, C., Swanson, C.J., and Hariadi, R.F. (2022). Viral aggregation: the knowns and unknowns. *Viruses* 14, 438. <https://doi.org/10.3390/v14020438>.
55. Kumru, O.S., Saleh-Birdjandi, S., Antunez, L.R., Sayeed, E., Robinson, D., van den Worm, S., Diemer, G.S., Perez, W., Caposio, P., Früh, K., et al. (2019). Stabilization and formulation of a recombinant Human Cytomegalovirus vector for use as a candidate HIV-1 vaccine. *Vaccine* 37, 6696–6706. <https://doi.org/10.1016/j.vaccine.2019.09.027>.